THE GAGA PROJECT: FROM THE IDEA TO A SUCCESSFUL SOUNDING ROCKET EXPERIMENT

Kirsten Harth, Stephan Höme, Torsten Trittel, Ulrike Kornek, Ulrike Strachauer, and Karl Will

Otto von Guericke University, 39106 Magdeburg, Germany

ABSTRACT

The rich phenomenology of granular matter is fascinating. Among the dynamic states of such materials is a highly diluted assembly referred to as granular gas. Here, we describe the preparation of a sounding rocket experiment on a granular gas of elongated grains, carried out within the REXUS / BEXUS (Rocket / Balloon Experiments for University Students) programme. From the birth of the idea in October 2009, through application and acceptance of the proposal in December 2009 and one year of design, construction and testing of the equipment, our team of four physicists and two engineers prepared a successful experiment for the REXUS 10 mission in February 2011 at ESRANGE, northern Sweden. The acquired experimental data are aimed to serve as a rich source for a qualitative understanding of the dynamics and statistics in Granular Anisotropic Gases (GAGa).

Key words: granular gas; sounding rocket; elongated particles; parabolic flight; micro-gravity; short range order; orientational correlations; orientation and velocity distribution.

1. INTRODUCTION

1.1. Granular Matter

Although most people have been familiar with granular materials since early childhood days, the physics of granular materials still supplies a vast amount of riddles. Solving these is of large importance in optimising industrial processes, understanding natural phenomena and improving the predictability of natural disasters. Although many phenomena have been described and understood, the search for a comprehensive dynamic theory of grainy materials is ongoing.

Granular materials represent loose ensembles of solid particles, uncountably many, and heavy enough so that they will not move unless mechanical energy is constantly supplied to them. They appear on all size scales - take for instance sand, rice, popcorn, loose boulders, the material in the Saturn rings. Depending on the excitation, different aggregate states are observed, similar to conventional materials. Because the grains are macroscopic, all collisions are dissipative and thermal fluctuations are irrelevant for the dynamics. Continouous energy supply is needed to maintain a fluidised or gaseous state. At constant excitation, a dynamic equilibrium establishes. The competition between dissipation and energy input can lead to pattern formation and counter-intuitive behaviour. For reviews on a large variety of such phenomena see, e.g., References [1, 2, 3, 4, 5, 6].

A granular gas is a dilute system of macroscopic particles interacting through inelastic collisions. In nature, granular gases are found, e.g., in snow- and landslides, in sandstorms or dust devils, in the formation and motion of dunes, in the planetary rings or the asteroid belt. Similar to molecular thermodynamics, a granular temperature can be defined from the mean square velocity of particles. The distribution of energy on the motional degrees of freedom can be calculated from the particle motion. To avoid sedimentation, either strong external forces (e.g. vibration [7, 8, 9, 10, 11, 12], electro-magnetic fields [13, 14]) or micro-gravity [15, 16, 17] are necessary in experiments.

Previous work concentrated on the dynamics of granular gases of spherical or completely irregular grains. There are many theoretical investigations of granular gases, but comparatively few experiments. Despite the superficial similarity to molecular gases, granular gases are essentially different: velocity distributions are non-Gaussian, equipartition of energy does not hold [18, 19] and clustering happens [20, 21, 22, 23], inelastic breakdown may occur [21, 24, 25]. The simplest theoretical description of a dissipative granular gas only considers collisions of ideally spherical particles, dissipation being usually described by the coefficient of restitution. Surface roughness of grains complicates the description and leads, e.g., to coupling and correlations between orientational and translational degrees of freedom [18, 26, 27].

In many of the existing experiments, granular gases are obtained by strong external excitation, mostly by vibration from the bottom of the container. As granular gases represent a system far from thermodynamic equilibrium, non-intuitive behaviour is frequently observed. For example, granular flux from compartments of low granular temperature to such of high granular temperature or sorting phenomena occur, see e.g. Ref. [6]. In many experiments, granular pressure, collision statistics, velocity

Proc. '20th ESA Symposium on European Rocket and Balloon Programmes and Related Research'
Hyère, France, 22–26 May 2011 (ESA SP-700, October 2011)

distributions, ergodicity and clustering, e.g., have been studied [7, 9, 15, 13, 14, 16, 17, 28, 29, 30, 31, 32, 33, 34]. Grains were levitated in all mentioned experiments. The systems were either continuously shaken or studied during granular cooling. Only one perspective view of the particle motion was monitored so that there is no 3D information on particle positions and velocities.

1.2. Anisotropic Particles and Orientational Order

When we refer to shape-anisotropic particles in the following, we mean elongated or flattened grains. The simplest examples are discs and rods - take for instance lentils or raw spaghetti. As is widely known from the molecular theory of liquid crystals [35] and as has been proven in nanoparticle [36, 37], bacteria or virous suspensions [38, 39, 40, 41], an anisotropic shape of the constituents of a fluid may lead to orientational order. In dry granulates, particles interact purely sterically. In particular, there is no long-range interaction potential (unlike electro-magnetic interactions in liquid crystals or hydrodynamic couplings in suspensions).
Vertical re-ordering from a horizontal ground state of rods in a thin vertically shaken cell has been observed by Ramaioli et al. [42]. Upright ordering and vortex motion is found for dense vertically vibrated rods in a container [43]. For more dilute ensembles, different ordered patterns form [44]. Quasi nematic, smectic and cubic states have been observed in vertically shaken monolayers [45]. In addition to the excitation strength, the aspect ratio (that is, the ratio of length and diametre of a particle) and the shape of the particle ends strongly influence the phase formation.

Aspelmeier et al. [46] study velocity distributions, energy decays and the formation, interaction and breakup of clusters in a non-confined one-dimensional granular gas of rodlike particles. Inelastic collapse is avoided in their simulations. Very recently, Kanzaki et al. [47] simulated the cooling of a non-confined granular gas of elongated particles in two dimensions, using Molecular Dynamics for soft particles. These authors particularly find large effects of particle shape and inelasticity on the cooling process. At strong dissipation and particle anisotropy, clusters possess an ordered quasi-nematic internal structure. There is no such study for a three-dimensional granular gas yet. So far, any experimental evidence is lacking.

1.3. The GAGa (Granular Anisotropic Gases) project

GAGa aims at the acquisition of three-dimensional experimental data of a granular gas of cylindrical elongated rods. The experiment was constructed for a sounding rocket mission. We intend to obtain a time-resolved statistics of the motion, the density distribution and orientational correlations of an ensemble of rods at different granular temperatures. Three-dimensional positions and orientations of rods are reconstructed from stereoscopic video camera views, and particles are tracked in consecutive frames. Here, we present our experiment design, preliminary measurements during parabolic flights and a short summary of the February 2011 sounding rocket experiment[1]. A snapshot of the granular anisotropic gas during the micro-gravity phase is shown in Fig 1. The evaluation of flight video data is still in progress, results will be reported elsewhere.

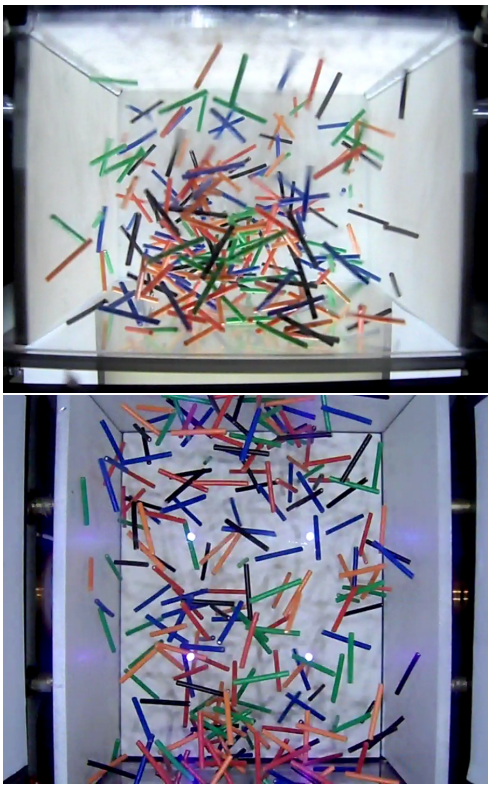

Figure 1. Snapshot of the granular anisotropic gas obtained on the REXUS 10 mission. Rods (diametre 1.2 mm, length 1.2 cm) are well distributed in the box, top (top, shaker front side corresponds to bottom in the image) and front view (bottom) of the container. Cameras are mounted upside down. The white spots are reflections of the illumination LEDs.

2. EXPERIMENT

The experimental setup consists of a mechanical, an optical and an electronic part. The whole equipment is mounted on an aluminium plate of 310 mm diametre, fixed to the bottom of a REXUS rocket-module of 350 mm outer diametre and 200 mm height, see Fig. 2.

[1] More background information, pre-flight and flight videos are available on www.gaga-in-space.de or on www.youtube.com/user/RexusGAGa; contact e-mail: kirsten.harth@ovgu.de

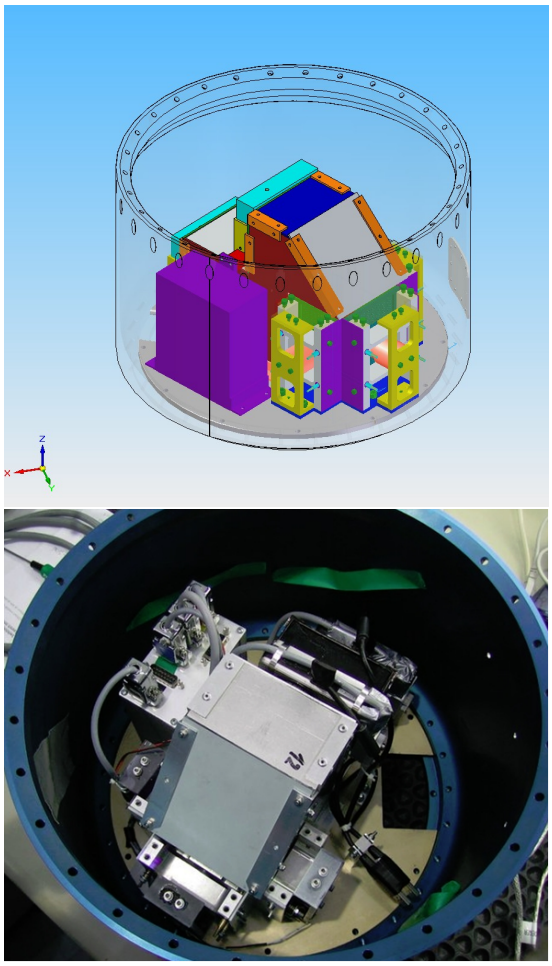

Figure 2. CAD-Drawing (top) and photo (bottom) of the final experiment design mounted in the REXUS 10 rocket module (350 mm outer diametre, 200 mm height). Setup components are shown in Fig. 3.

The experiment runs autonomously, uplink to the rocket is not available during flight.

2.1. Mechanical setup

All mechanical parts of the setup are self designed and constructed. The main parts are a box with moveable wall plates (shaker), two camera mounts, an optical tunnel to avoid stray light and a box containing the electronics, see Fig. 3.

The shaker is confined by an aluminium ground plate, plexiglass top and front plates and three moveable aluminium plates, see Fig. 4a. The inner dimensions of the box are 100 mm × 80 mm × 60 mm ($h \times w \times d$), when the moveable plates are in inner position. Well-defined central positions of the moveable plates are implemented by four pressure springs, each mounted on a brass guide bolt, see Fig. 4b. Walls are driven separately by

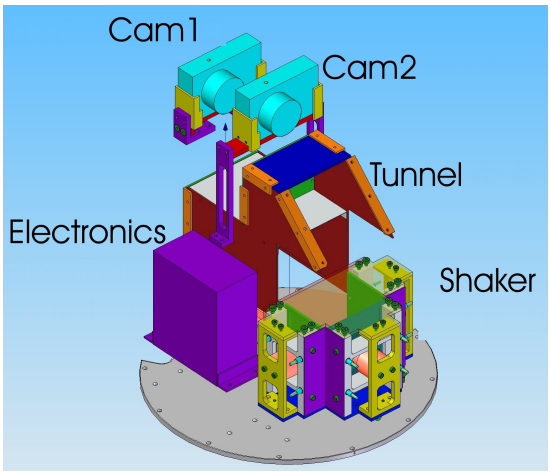

Figure 3. Exploded drawing of the GAGa setup. The main parts are the shaker, an optical tunnel, two mounted cameras and one box for the electronics.

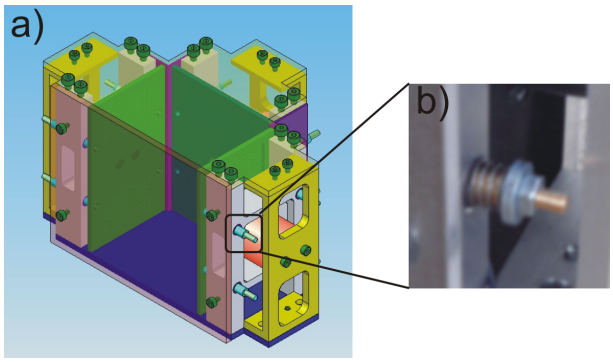

Figure 4. a) CAD-drawing of the box with moveable walls; b) detail photo of a mounted pressure spring to realise a defined central position of the moveable walls.

voice-coil actuators AVM 30-15 (A-Drive technologies).

The optical tunnel is made of aluminium plates. Two holes (d=45 mm) in the tunnel back plates are left for the camera lenses. The cameras are fixed to aluminium profiles using stainless steel zip ties. The bottom camera (Cam1) is mounted at a distance of 155 mm and the top camera (Cam2) at a distance of 65 mm to the plexiglass front plate of the shaker. These distances are essentially determined by the spatial restrictions of the rocket module and an optimal field of view in the upper camera video.

2.2. Optical setup

The shaker is illuminated with four LXM3-PW71 high power LEDs (PHILIPS LUMILEDS) placed around the bottom camera lens on the lower optical tunnel back plate, see Fig. 5. Videos of the experiment are recorded with two commercial Samsung PL70 CCD-cameras with

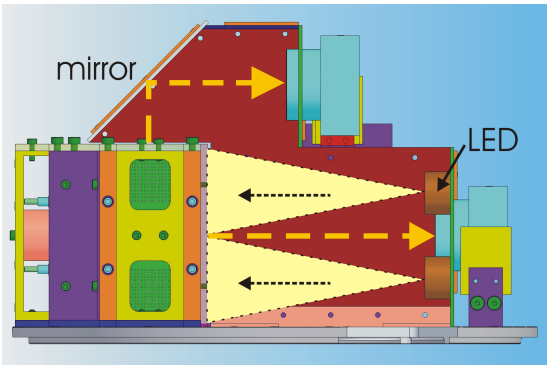

Figure 5. Impinging light-system with four LEDs positioned in a rectangle around the hole for the bottom camera lens in the tunnel back wall. All metal parts in the tunnel were flat coloured and anti-reflection coated plexiglass was used for translucent shaker walls.

SD-card storage. The frame-rate is approximately 30 fps at 1280 pixel x 720 pixel. This corresponds to a spatial resolution of about 0.14 mm/pixel in the middle plane of the box. During testing, experiment videos can be downloaded and removed via a camera USB port accessible through a hatch in the module. Due to spatial restrictions, cameras are installed upside down.
The bottom camera directly views the front of the box. In contrast, the top camera views a projection of the top of the box on a plane mirror, mounted in the tunnel above the box at an angle of 45°. To minimise reflections in the setup, we use anti-reflection coated plexiglass for the shaker top and front plates. The aluminium walls of the shaker were painted flat white, no unpainted metal piece was left in the optical tunnel.

2.3. Electronics

Several parts of the setup must be controlled according to a pre-defined timeline. Additionally, a communication link to the ground-station is established via the rocket service system, providing diagnostic data during testing and flight.

In order to encapsulate time-critical functions (communication, signal generation), a dual-controller-setup was chosen. The Communication and Control Unit (CCU - Atmel ATmega 32) manages the timeline as well as communication with the rocket service system. Additionally, this unit provides the digital signals to control cameras and LEDs. The Shaker Control Unit (SCU - Atmel ATtiny 2313) generates the signals for the voice coil actuators. The power supply unit (PSU) transforms the rocket battery voltage into galvanically isolated, stabilised voltages for the experiment components. A ground control software to monitor and control the experiment during testing, pre-flight and flight phase was developed.

Communication and Control Unit (CCU).
The CCU manages all steps during the experiment with an internal timeline. The internal timer is triggered with the lift-off signal from the rocket service system. According to the programmed schedule, the timeline module then invokes the control-functions for the peripherals and sends signals to the SCU.
The rocket service system provides an RS-422 interface for the downlink to the ground control station. This is connected to the CCU micro-controller. To monitor the state of the experiment, a diagnostic telegram containing the internal time, current status of state machines and peripheral information is transmitted from the experiment to the ground station every second. Some commands (reset, start of experiment, camera control commands) can be sent to the CCU for testing purposes if an uplink is installed.
The current for the LEDs is provided by linear voltage converters in constant current wiring. The voltage converters provide an enable-pin, which is used to switch the LEDs on and off.
The cameras are consumer products, therefore there is no special interface or software to control them provided by the manufacturer. For this reason, they were partly disassembled and push-buttons were replaced by wires soldered to switching transistors. Thus, the CCU can 'press' the buttons of the cameras to switch power, to focus and to start or stop recording. The state of the cameras is monitored by measuring the voltage at the status led.

Shaker Control Unit (SCU).
During the experiment, the voice coil actors are driven with a sine signal of variable frequencies and amplitudes. We achieve this using one full-bridge driver designed for motor-controlling each vibrating plate. The SCU generates a pulse width modulation signal at 16 kHz. A sine signal with a frequency of 20 Hz or 30 Hz is modulated onto the carrier. As 16 kHz is way above the time constants of the mechanical system, the voice coils move like a sine function.

Power Supply Unit (PSU).
The power supply scheme of GAGa is presented in Fig. 6. The rocket service system delivers a voltage level of 24...36V. The experiment uses two voltage levels, +5V DC and +24V DC. Both are generated by step-down switching power modules (Tracopower THD-15 series).
Voice coil actuators are supplied with +24V, the microcontrollers and the LEDs operate at +5V supply voltage. The 4V voltage for the cameras is generated out of the 5V rail using linear voltage converters.

Ground Control.
The ground control software receives the telegrams generated by the CCU via a serial port and decodes them. The status of the experiment is visualised with coloured indicators and text messages. The ground control software records the raw data streams over the communication link as well as the decoded status messages for detailed debugging during the testing phase and in case of an experiment failure during flight. For testing purposes, several commands can be sent to the experiment if an uplink is available.

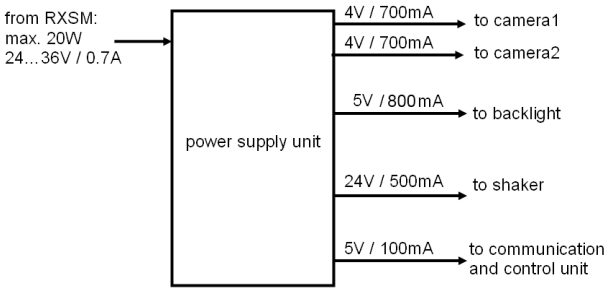

Figure 6. Power supply scheme of the GAGa experiment: In the PSU, the level from service module power supply (left) is converted to the voltage levels of the separate experiment components (right).

2.4. Testing

In preparation of the rocket flight, the setup passed two major tests, a thermal vacuum test (TVT) and a vibration test. Different testing conditions for the TVT were: first, temperature -20°C and pressure less than 0.5 mbar for ... minutes; second, temperature 50°C pressure less than 0.5 mbar for ... minutes; and third an ascend simulation (room temperature, the pressure is reduced from 1 bar to 1 mbar within 70 s and reverse). Prior to this, the cameras were vacuum-tested separately in the lab. For the vibration test, the setup was shaken in the x-, y- and z-directions at the acceptance level of 6g root mean square noise. Resonance curves of the setup before and after each test run were compared for analysis. Standard benchmark-, integration- and interference-tests were performed prior to campaign.

2.5. Experiment description

The shaker is filled with 250 cylindrical colored rods (length 12 mm; diametre 1.2 mm). This corresponds to $\sim 3\%$ of the inner shaker volume. An internal clock to time all further actions of the experiment is triggered with the rocket lift off signal. Eighty seconds after lift off (early zero g phase), the moveable plates start shaking at a frequency of $f = 30\,\mathrm{Hz}$ and an amplitude $A = \pm 1\,\mathrm{mm}$ around their central positions. At 90 seconds, we switch on the LEDs and start video recording. 151 seconds after lift off the shaker frequency is changed to $f = 20\,\mathrm{Hz}$ and the shaker amplitude to $A = \pm 1.2\,\mathrm{mm}$. Thus, the second phase should provide less excitation of the rods. At the end of the zero g phase (225 s), the CCU starts the shut down procedure (stop shaking, switch off LEDs, save video on memory card, switch off cameras).

3. PARABOLIC FLIGHTS

In preparation of the REXUS 10 experiment, we took part in the 15th and 16th DLR parabolic flight campaigns in Bordeaux. These two campaigns turned out to be crucial for the final success of our rocket experiment, because they answered many open questions, and we could identify and eliminate technical problems. We were able to test the components and we optimised experimental parameters to match our requirements.

Figure 7. Two snapshots of 250 (left) and about 1000 (right) rods moving in a $10 \times 10 \times 10\,\mathrm{cm}^3$ plexiglass container during a low-acceleration period on a parabolic flight.

During the 15th campaign in March 2010, we considered the basic functionality of the excitation technique, the selection of particles, excitation frequencies and amplitudes. We constructed two simple prototypes.
The first one was placed in a rack. It consisted of a $10 \times 10 \times 10\,\mathrm{cm}^3$ plexiglass box, one digital camera and a shaking metal baseplate. We used a commercial loudspeaker as actuator and glued the baseplate to the membrane. Frequency (10-60 Hz) and amplitude (up to about 2 mm) were computer controlled with a Labview programme. All container walls but the back side were translucent. A video was taken in front view. Our particles were hand-cut aluminium wire pieces of 1 cm length and 1 mm diametre. There were approximately 250 pieces in the box. Between different flight days, it was not possible to change the number of particles in the box. As expected, the remaining acceleration in the aircraft (g-jitter) was too strong to obtain experimental data of satisfactory quality. The granulate was pushed against one of the side walls most of the time, the vibrating baseplate not affecting the particles any longer. In the subsequent flight we tested a free-floating box with about 1000 rods instead of a shaker fixed to the rack, but the quality of micro-gravity was not sufficient either.

Fig. 7 shows snapshots of the rods in the box. From the video data, it is evident that rods swirl around at a lower volume fraction (250 rods), while they strongly interact among each other and with the walls in short periods of rod motion at higher volume fraction (1000 rods). However, at the high volume fraction we would not track rods in 3D, and the video quality obtained on the parabolic flight is insufficient to allow for a detailed analysis of rod motion. Despite the insufficient zero-g quality, we were able to improve our design for the rocket flight essentially. Most important, we had to improve the optics: Optical reflections at the box and rod surfaces deteriorated the image quality. The box was re-designed using anti-reflection coated plexiglass. All non-translucent parts were flat coloured. The bare wire-pieces were replaced by non-reflecting coloured

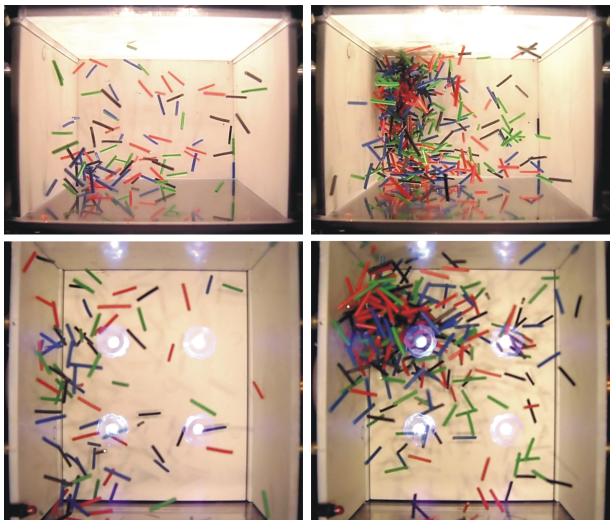

Figure 8. Snapshots of 120 (left) and 400 (right) rods moving in the container during a low g-jitter phase during a parabolic flight. Cameras are mounted upside down. Upper panel: top camera, shaker front side corresponds to bottom of the images; lower panel: bottom camera.

rods. The camera was connected to the shaking box by an optical tunnel with non-reflecting walls. The experiments confirmed that the choice of camera-type was satisfactorily, in terms of frame-rate, shutter times and spatial resolution. In lab experiments, we found that dark rods in front of white walls give the best contrast. As a consequence of the observations during the first parabolic flight test, the chamber was equipped with three vibrating walls, instead of two in the preliminary design.

During the 16th DLR parabolic flight campaign in November 2010, we were able to test our flight-ready setup for REXUS 10. The aim of this flight was a final optimisation of experimental parameters. The setup worked autonomously, so amplitudes and frequencies were fixed prior to the campaign. The sample consisted of 1 cm long, 1.2 mm diametre red, green, black and blue coated copper wire. Videos were recorded in rocket flight configuration, with two cameras from perpendicular perspectives. We tested four different situations: 120 rods or 400 rods in the box, each sample shaken at 10 Hz or 30 Hz. The box was front-illuminated with four LEDs with wide-angle lenses attached to them. The brightness of the illumination in this configuration is higher than with bare LEDs, but despite the anti-reflection coating the shapes of the lenses and holders strongly reflect on the shaker front wall, Fig. 8. Thus, the LED lenses were removed to maximise the evaluable part of the video images in the rocket experiments, leaving only four small white spots as the reflection of the LEDs in the images, see Fig. 1.

Figure 8 shows typical images of the particles in the container taken from the video sequences. At 30 Hz, particles are well pushed away from the walls. Their velocity is high, but still in a range where they can be tracked in consecutive video frames. At 10 Hz (and higher amplitude), the forcing becomes more inefficient. We found that 120 particles are too little as their mean free path becomes close to the box dimensions - inter-particle interactions are rare. 400 particles are too many to guarantee a reliable tracking and rod identification. The problem of g-jitter persisted, but due to rod agitation from three sides the excitation was more efficient than at the previous parabolic flight campaign.
From the videos taken during the micro-gravity phase, we concluded that the best parameter set would be shaking frequencies of 20 and 30 Hz. In order to assure a sufficient rate of inter-particle collisions, we chose 250 rods of 1.2 cm length on the REXUS 10 flight.

4. ROCKET FLIGHT SUMMARY

The conditions on the REXUS 10 flight were ideal for our experiment: we were positioned close to center of gravity, and the rocket was spinning at only $\approx$3 deg/s during the zero-g. This yielded great experiment conditions. During flight, we received all scheduled signals. From the evaluation of the videos on the camera SD cards, we find that the experiment performed fine. We met most requirements for our experiment and got good data from the flight. Our granulate was well distributed in the container during approximately the first 110 s of the recording period, see Fig. 1. After that, the micro-gravity quality diminished drastically so that large amounts of rods were situated near a container wall, comparable to the parabolic flight results. The number of the rods as well as the chosen excitation frequencies and amplitudes were fine. Shaking of the third (back) container wall led to an increased density of rods close to the front wall, which was not intended. We did not encounter problems resulting from electric charges on the rods. The video quality of the upper camera is lower than for the bottom camera due to less illumination. Videos are not exactly synchronous. Both was expected, and videos will be useable. A final setup evaluation will be only possible after a complete data analysis, which is currently in progress.

5. SUMMARY

We reported our experiences in the REXUS 10 project GAGa (Granular Anisotropic Gases), from the very beginning to a successful experiment on flight. The experimental design is presented in its final form. We present preliminary data from two parabolic flight campaigns. These are evaluated in accordance with experiment requirements and show exemplarily that the micro-gravity quality on such flights is insufficient to obtain experimental data in our setup configuration. However, an experiment optimisation would not have been possible without

these test runs. As expected, rods perform seemingly unordered swirling motions at low volume fraction. Due to the bad video data quality from the first parabolic flight, this phenomenon has not been investigated in detail. Finally, the raw experimental results of the GAGa experiment on the REXUS 10 mission in February 2011 are summarised. The rods are well distributed in the container, interactions occur frequently and the video quality is sufficient for data evaluation. A detailed analysis is in progress, results will be reported elsewhere.

ACKNOWLEDGMENTS

The authors cordially thank Prof. Ralf Stannarius for his passionate support - from the birth of the idea to the final data evaluation, for the opportunity to take part in two parabolic flights and for critical reading of this manuscript. The GAGa team is indebted to Prof. Christian Diedrich for continuously supporting the project. Frank Rietz and David Fischer significantly contributed to the early experiment conception. Thomas John and Sebastian Baumgarten are acknowledged for their support in the integration of the experiment and for carrying out several test runs during flight. The GAGa team thanks Martin Schünemann for finite elements structure analysis of some experiment components. Tilo Finger is acknowledged for his help in carrying out test experiments on granular flows prior to project acceptance.
Last but not least, we thank the whole REXUS / BEXUS team of DLR and ESA, especially Mark Fittock, Martin Siegl and Andreas Stamminger for their great project organisation and steady support during the whole project. We thank Olle Persson for spreading motivation and enthusiasm, and him and our payload manager Mark Uitendaal for a great campaign Sweden. We thank DLR Moraba and the SSC crew for a successful rocket mission.
The GAGa project was funded by DLR / ESA / SNSB within the REXUS / BEXUS programme. Our attendance of the 15th and 16th DLR parabolic flight campaigns was funded within the DLR Grant OASIS-CO. We thank the Faculty of Natural Sciences and the administration of the Otto-von-Guericke University Magdeburg for financial support.

REFERENCES

[1] T. Poeschel and I. Luding (ed). *Granular Gases*. Springer, Berlin, 2001.

[2] I. S. Aranson and L. S. Tsimring. *Granular Patterns*. Oxford University Press, Oxford, 2009.

[3] H. M. Jaeger, S. R. Nagel, and R. P. Behringer. Granular soildis, liquids, and gases. *Rev. Mod. Phys.*, 68:1259–1273, 1996.

[4] D. Beysens and P. Evesque. Vibrational phenomena in near-critical fluids and granular matter. *Topical Teams in the Life and Physical Sciences*, SP-1281:6–21, 2005.

Figure 9. The GAGa team in front of the REXUS 10 rocket at ESRANGE, shortly before launch, 23rd February 2011 (from left to right: U. Strachauer, K. Harth, S. Höme, U. Kornek, T. Trittel, K. Will).

[5] I. S. Aranson and L. S. Tsimring. Patterns and collective behaviour in granular media: Theoretical concepts. *Rev. Mod. Phys.*, 78:641–692, 2006.

[6] K. van der Weele. Granular gas dynamics: how maxwell's demon rules in a non-equilibrium system. *Cont. Phys.*, 49:157–178, 2008.

[7] F. Rouyer and N. Menon. Velocity fluctuations in a homogeneous 2d granular gas in steady state. *Phys. Rev. Lett.*, 85:3676–3679, 2000.

[8] J. S. Olafsen and J. S. Urbach. Velocity distributions and density fluctuations in a granular gas. *Phys. Rev. E*, 60:R2468–R2471, 1999.

[9] J. S. Olafsen and J. S. Urbach. Clustering, order, and collapse in a driven granular monolayer. *Phys. Rev. Lett.*, 81:4369–4372, 1998.

[10] R. Mikkelsen, D. van der Meer, K. van der Weele, and D. Lohse. Competitive clustering in a bidisperse granular gas: experiment, molecular dynamics, and flux model. *Phys. Rev. E*, 70:061307, 2004.

[11] R. Mikkelsen, D. van der Meer, K. van der Weele, and D. Lohse. Competitive clustering in a granular gas. *Phys. Fluids*, 159:S8, 2003.

[12] S. Viridi, M. Schmick, and M. Markus. *Phys. Rev. E*, 74:041301, 2006.

[13] C. C. Maaß, N. Isert, G. Maret, and C. M. Aegerter. Experimental investigation of the freely cooling granular gas. *Phys. Rev. Lett.*, 100:248001, 2008.

[14] I. S. Aranson and J. S. Olafsen. Velocity fluctuations in electrostatically driven granular media. *Phys. Rev. E*, 66:061302, 2002.

[15] P. Evesque, F. Palencia, C. Lecoutre-Chabot, D. Beysens, and Y. Garrabos. Granular gas in weightlessness: The limit case of very low densities of non interacting spheres. *Microgravity Sci. Technol.*, XIV-I:280–284, 2005.

[16] E. Falcon, R. Wunenburger, P. Evesque, S. Fauve, C. Chabot, Y. Garrabos, and D. Beysens. Cluster

formation in a granular medium fluidized by vibrations in low gravity. *Phys. Rev. Lett.*, 83:440–443, 1999.

[17] E. Falcon, S. Aumaitre, P. Evesque, F. Palencia, C. Lecoutre-Chabot, S. Fauve, D. Beysens, and Y. Garrabos. Collision statistics in a dilute granular gas fluidized by vibrations in low gravity. *Eur. Phys. Lett.*, 74:830–836, 2006.

[18] M. Huthmann and A. Zippelius. Dynamics of inelastically colliding rough spheres: Relaxation of translational and rotational energy. *Phys. Rev. E*, 56:R6275–R6277, 1997.

[19] S. Luding, M. Huthmann, S. McNamara, and A. Zippelius. Homogeneous cooling of rough, dissipative particles: Theory and simulations. *Phys. Rev. E*, 58:3416–3425, 1998.

[20] I. Goldhirsch and G. Zanetti. Clustering instability in dissipative gases. *Phys. Rev. Lett.*, 70:1619–1622, 1993.

[21] S. McNamara and W. R. Young. Inelastic collapse and clumping in a one-dimensional granular medium. *Phys. Fluids A*, 4:504, 1992.

[22] R. Brito and M. H. Ernst. Extension of haff's cooling law in granular flows. *Europhys. Lett.*, 43:497–502, 1998.

[23] S. Miller and S. Luding. Cluster growth in two- and three-dimensional granular gases. *Phys. Rev. E*, 69:031305, 2004.

[24] S. McNamara and W. R. Young. Dynamics of a freely eveolving, two-dimensional granular medium. *Phys. Rev. E*, 53:5089–5100, 1996.

[25] A. Barrat, E. Trizac, and M. H. Ernst. Granular gases: dynamics and collective effects. *J. Phys.: Cond. Matter*, 17:S2429–S2437, 2005.

[26] N. V. Brilliantov, T. Pöschel, W. T. Kranz, and A. Zippelius. Translations and rotations are correlated in granular gases. *Phys. Rev. Lett.*, 98:128001, 2007.

[27] B. Gayen and M. Alam. Orientational correlation and velocity distributions in uniform shear flow of a dilute granular gas. *Phys. Rev. Lett.*, 100:068002, 2008.

[28] J. J. Brey and M. J. Ruiz-Montero. Velocity distributions of fluidized granular gases in the presence of gravity. *Phys. Rev. E*, 67:021307, 2003.

[29] S. J. Moon, J. B. Swift, and H. L. Swinney. Steady-state velocity distributions of an oscillated granular gas. *Phys. Rev. E*, 69:011301, 2004.

[30] M. Hou, R. Liu, G. Zhai, Z. Sun, K. Lu, Y. Garrabos, and P. Evesque. Velocity distribution of vibration-driven granular gas in knudsen regime in microgravity. *Micrograv. Sci. Technol.*, 20:73–80, 2008.

[31] X. Nie, E. Ben-Naim, and S. Chen. Dynamics of freely cooling granular gases. *Phys. Rev. Lett.*, 89:204301, 2002.

[32] T. P. C. van Noije and M. H. Ernst. Velocity distributions in homogeneous granular fluids: the free and the heated case. *Granular Matter*, 1:57–64, 1998.

[33] M. Leconte, Y. Garrabos, E. Falcon, C. Lecoutre, F. Palencia, P. Evesque, and D. Beysens. *J. Stat. Mech.*, page P07012, 2006.

[34] M. Leconte, Y. Garrabos, C. Lecoutre, F. Palencia, P. Evesque, and D. Beysens. *Appl. Phys. Lett.*, 89:243518, 2006.

[35] P. G. de Gennes and J. Prost. *The Physics of Liquid Crystals*. Clarendon Press, Oxford, 1993.

[36] A. Eremin, R. Stannarius, S. Klein, J. Heuer, and R. M. Richardson. Switching of electrically responsive, light-sensitive colloidal suspensions of anisotropic pigment particles. *Anv. Func. Materials*, 21:566, 2011.

[37] D. van der Beek, H. Reich, P. van der Schoot, M. Dijkstra, T. Schilling, R. Vink, M. Schmidt, R. van Roij, and H. Lekkerkerker. Isotropic-nematic interface and wetting in suspensions of colloidal platelets. *Phys. Rev. Lett.*, 97:087801, 2006.

[38] F. Peruani, A. Deutsch, and M. Bär. Nonequilibrium clustering of self-propelled rods. *Phys. Rev. E*, 74:030904(R), 2006.

[39] H. Chate, F. Ginelli, and R. Montange. Simple model for active nematics: quasi-long-range order and giant fluctuations. *Phys. Rev. Lett.*, 96:180602, 2006.

[40] A. Kudrolli, G. Lumay, D. Volfson, and L. S. Tsimring. Swarming and swirling in self-propelled granular rods. *Phys. Rev. Lett.*, 100:058001, 2008.

[41] M. P. Lettinga and J. K. G. Dhont. Non-equilibrium phase behaviour of rod-like viruses under shear flow. *J. Phys. Condens. Matter*, 16:3929, 2004.

[42] M. Ramaioli, L. Pournin, and T. M. Liebing. Vertical ordering of rods under vertical vibration. *Phys. Rev. E*, 76:021304, 2007.

[43] D. L. Blair, T. Neicu, and A. Kudrolli. Vortices in vibrated granular rods. *Phys. Rev. E*, 67:031303, 2003.

[44] J. Galanis, D. Harries, D. L. Sackett, W. Losert, and R. Nossal. Spontaneous patterning of confined granular rods. *Phys. Rev. Lett.*, 96:028002, 2006.

[45] V. Narayan, N. Menon, and S. Ramaswamy. Nonequilibrium steady states in a vibrated-rod monolayer: tetratic, nematic and smectic correlations. *J. Stat. Mech.*, 01:P01005, 2006.

[46] T. Aspelmeier, G. Giese, and A. Zippelius. Cooling dynamics of a dilute gas of inelastic rods: A many particle simulation. *Phys. Rev. E*, 57:857–865, 1998.

[47] T. Kanzaki, R. C. Hidalgo, D. Maza, and I. Pagonabarraga. Colling dynamics of a granular gas of elongated particles. *J. Stat. Mech.*, 06:P06020, 2010.